

1  
2 **Responses of globally important phytoplankton species to olivine dissolution products and**  
3 **implications for carbon dioxide removal via ocean alkalinity enhancement**  
4  
5  
6  
7  
8  
9  
10  
11

12 David A. Hutchins<sup>1†\*</sup>, Fei-Xue Fu<sup>1</sup>, Shun-Chung Yang<sup>1</sup>, Seth G. John<sup>1</sup>, Stephen J. Romaniello<sup>2</sup>,  
13 M. Grace Andrews<sup>2</sup>, Nathan G. Walworth<sup>1,2,3†\*</sup>

14  
15  
16  
17  
18  
19  
20  
21  
22  
23  
24  
25  
26  
27  
28  
29 <sup>1</sup>University of Southern California, Los Angeles, CA, USA

30 <sup>2</sup>Vesta, PBC, San Francisco, CA, USA

31 <sup>3</sup>J. Craig Venter Institute, La Jolla, CA, USA

32  
33 †These authors contributed equally to this work

34 \*Correspondence: David A. Hutchins - [dahutch@usc.edu](mailto:dahutch@usc.edu), Nathan G. Walworth –  
35 [nate@vesta.earth](mailto:nate@vesta.earth)

36

37  
38  
39  
40  
41  
42  
43  
44  
45  
46  
47  
48  
49  
50  
51  
52  
53  
54  
55  
56  
57  
58  
59  
60  
61  
62  
63  
64  
65  
66  
67  
68

**Abstract**

Anthropogenic greenhouse gas emissions are leading to global temperature increases, ocean acidification, and significant ecosystem impacts. Given current emissions trajectories, the IPCC reports indicate that rapid abatement of CO<sub>2</sub> emissions and development of carbon dioxide removal (CDR) strategies are needed to address legacy and difficult to abate emissions sources. These CDR methods must efficiently and safely sequester gigatons of atmospheric CO<sub>2</sub>. Coastal Enhanced Weathering (CEW) via the addition of the common mineral olivine to coastal waters is one promising approach to enhance ocean alkalinity for large-scale CDR. As olivine weathers, it releases several biologically active dissolution products, including alkalinity, trace metals, and the nutrient silicate. Released trace metals can serve as micronutrients but may also be toxic at high concentrations to marine biota including phytoplankton that lie at the base of marine food webs. We grew six species representing several globally important phytoplankton species under elevated concentrations of olivine dissolution products via a synthetic olivine leachate (OL) based on olivine elemental composition. We monitored their physiological and biogeochemical responses, which allowed us to determine physiological impacts and thresholds at elevated olivine leachate concentrations, in addition to individual effects of specific constituents. We found both positive and neutral responses but no evident toxic effects for two silicifying diatoms, a calcifying coccolithophore, and three cyanobacteria. In both single and competitive co-cultures, silicifiers and calcifiers benefited from olivine dissolution products like iron and silicate or enhanced alkalinity, respectively. The non-N<sub>2</sub>-fixing picocyanobacterium could use synthetic olivine-derived iron for growth, while N<sub>2</sub>-fixing cyanobacteria could not. However, other trace metals like nickel and cobalt supported cyanobacterial growth across both groups. Growth benefits to phytoplankton groups *in situ* will depend on species-specific responses and ambient concentrations of other required nutrients. Results suggest olivine dissolution products appear unlikely to cause negative physiological effects for any of the phytoplankton examined, even at high concentrations, and may support growth of particular taxa under some conditions. Future studies can shed light on long-term eco-evolutionary responses to olivine exposure and on the potential effects that marine microbes may in turn have on olivine dissolution rates and regional biogeochemistry.

## 69 Introduction

70

71 Excess anthropogenic greenhouse gas emissions are driving global changes to Earth  
72 systems and leading to simultaneous increases in sea surface temperatures, ocean acidification,  
73 and regional shifts in nutrient supplies (IPCC, 2022). To counteract these trends and limit the  
74 average global temperature increase to 1.5-2°C, carbon dioxide removal (CDR) methods that can  
75 collectively remove and permanently store gigatons of atmospheric CO<sub>2</sub> (GtCO<sub>2</sub>) must be  
76 developed (Rogelj et al., 2018). Coastal Enhanced Weathering (CEW) with olivine (Mg<sub>2</sub>-  
77 <sub>x</sub>Fe<sub>x</sub>SiO<sub>4</sub>) has been proposed as an economically scalable form of ocean alkalinity enhancement  
78 (OAE), as it is a globally abundant, naturally occurring ultramafic silicate mineral (Taylor et al.,  
79 2016; Caserini et al., 2022). Olivine is considered to be one of the most favorable minerals for  
80 CDR as it weathers quickly under Earth surface conditions (Oelkers et al., 2018). Like other  
81 silicate minerals, it dissolves in water to release cations (Mg<sup>2+</sup>, Fe<sup>2+</sup>) and generates alkalinity  
82 (principally HCO<sub>3</sub><sup>-</sup>), with up to 4 mol of CO<sub>2</sub> sequestered per mol of olivine [Eq. 1].

83



85

86 Forsteritic olivine is the magnesium-rich end-member of olivine and can contain various other  
87 trace constituents. For example, olivine used in this study contains ~92% magnesium (Mg<sup>2+</sup>) and  
88 ~8% ferrous iron (Fe<sup>2+</sup>) along with trace amounts (<1%) of other metals such as nickel (Ni),  
89 chromium (Cr), and cobalt (Co). As olivine weathers, it releases several biologically important  
90 dissolution products into the surrounding seawater: (I) bicarbonate (HCO<sub>3</sub><sup>-</sup>) and carbonate ion  
91 (CO<sub>3</sub><sup>2-</sup>), hereafter summarized as “alkalinity”; (II) silicic acid (Si(OH)<sub>4</sub>) hereafter termed  
92 silicate; (III) and a variety of trace metals including iron (Fe<sup>2+</sup>, or oxidized aqueous species),  
93 nickel (Ni<sup>2+</sup>), cobalt (Co<sup>2+</sup>), and chromium (CrVI). These dissolution products have the potential  
94 to affect important phytoplankton functional groups like silicifying algae (diatoms), calcifying  
95 algae (coccolithophores), and cyanobacteria, which lie at the base of marine food webs and drive  
96 the biological carbon pump (Hauck et al., 2016; Moran, 2015). Hence, it is important to  
97 understand the specific effects of these constituents on globally important phytoplankton species,  
98 particularly at elevated concentrations to simulate large-scale CEW applications.

99

100 Significant alkalinity additions from olivine weathering can consume CO<sub>2</sub> from the  
101 surrounding seawater, causing a CO<sub>2</sub> deficit until air-sea equilibration. This shift in the carbonate  
102 system from CO<sub>2</sub> to HCO<sub>3</sub><sup>-</sup>/CO<sub>3</sub><sup>2-</sup> by transient, non-equilibrated OAE may affect phytoplankton  
103 functional groups differently, with some taxa being more sensitive than others. For example, it is  
104 predicted that calcifying organisms like coccolithophores may benefit from CEW due to  
105 decreases in proton concentrations (H<sup>+</sup>) and increases in the CaCO<sub>3</sub> saturation state.  
106 Additionally, dissolving one mole of olivine leads to a one mole increase in dissolved silicate,  
107 which is an essential and often bio-limiting nutrient for silicifying organisms like diatoms, a  
108 phytoplankton group estimated to contribute up to 40% of the marine primary production  
(Bertrand et al., 2012). Hence, diatoms may especially benefit from CEW applications with

109 olivine. Additionally, diatoms are particularly noted for being dominant phytoplankton in the  
110 coastal regimes where olivine deployments are likely to take place (Field et al., 1998). While  
111 there are both planktonic and benthic species of diatoms, the latter will presumably be exposed to  
112 especially sustained and elevated levels of dissolution products when olivine is deployed in  
113 natural marine sediments. It is unknown if either group, calcifiers or silicifiers, may consistently  
114 outcompete the other following CEW with olivine (Bach et al., 2019).

115 Trace metals like Fe and Ni are general micronutrients required by all classes of  
116 phytoplankton and could potentially support their growth upon fluxes into seawater from olivine  
117 weathering. In particular, dinitrogen (N<sub>2</sub>)-fixing cyanobacteria and diatoms both have elevated  
118 Fe requirements (Hutchins and Sañudo-Wilhelmy, 2021; Hutchins and Boyd, 2016), and so may  
119 stand to benefit from increases in Fe concentrations. Although a required micronutrient at low  
120 levels, in high enough concentrations Ni may potentially negatively impact phytoplankton  
121 growth, although one recent study showed limited to no toxic effects of very high Ni  
122 concentrations (e.g. 50,000 nmol L<sup>-1</sup>) for several phytoplankton taxa (Guo et al., 2022). Cobalt  
123 can also serve as a micronutrient for phytoplankton (Sunda and Huntsman, 1995; Hawco et al.,  
124 2020) but may also be toxic at high concentrations (Karthikeyan et al., 2019). However, other  
125 trace metals found with olivine such as Cr are not nutrient elements and also need to be  
126 considered in terms of their possible toxicity to phytoplankton (Flipkens et al., 2021; Frey et al.,  
127 1983).

128 Hence, it is important to understand the taxon-specific effects of these constituents to  
129 determine thresholds at which key phytoplankton functional groups may experience positive or  
130 negative effects. Furthermore, it is important to expose phytoplankton to elevated concentrations  
131 of olivine dissolution products simultaneously to understand what impacts may occur for large  
132 CEW applications. Exposures of organisms to concentrated olivine dissolution products also  
133 provides an “worst case scenario” benchmark, which can be compared to lower actual  
134 environmental exposures resulting from small CEW additions, slower olivine dissolution time  
135 scales, and dilution from advection. While olivine weathers relatively quickly compared to other  
136 silicate minerals (Hartmann et al., 2013), dissolution of olivine grains is gradual (i.e. years)  
137 relative to microbial physiological responses (hours), posing a challenge to test different  
138 concentrations of olivine constituents on phytoplankton physiology. To address this, we prepared  
139 a synthetic olivine leachate (OL) composed of olivine dissolution products with trace metal  
140 concentrations well over those of seawater (7-12,000 times higher), in order to represent a “worst  
141 case” scenario for a CEW project. This extreme scenario was estimated based on the maximum  
142 expected impact of olivine weathering on the chemistry of the overlying water column.  
143 Assuming a 10 cm thick layer of pure olivine sand dissolves with a 100 year half-life into 1  
144 meter of overlying water with a 24 hour residence time, the anticipated steady state change in the  
145 alkalinity of the overlying water column is 65 umol/kg (assuming 4 moles of alkalinity per mole  
146 olivine (Meysman and Montserrat, 2017) and 100% release to the water column). The  
147 concentrations of other components were chosen assuming stoichiometric, congruent dissolution  
148 and quantitative release to the water column as well -- a worst case scenario. Furthermore,

149 phytoplankton were exposed to OL within a small, enclosed batch culture. We cultured 6 species  
150 representing three globally important phytoplankton functional groups: 2 diatoms (*Nitzschia*,  
151 *Ditylum*), 1 coccolithophore (*Emiliana*), 2 dinitrogen (N<sub>2</sub>) fixing cyanobacteria (*Trichodesmium*,  
152 *Crocospaera*), and 1 non-N<sub>2</sub> fixing picocyanobacterium (*Synechococcus*). All of these species  
153 are planktonic, with the exception of the diatom *Nitzschia* which frequently forms benthic  
154 biofilms (Yamamoto et al., 2008). Cultures were grown semi-continuously in natural seawater  
155 based modified Aquil media (Sunda et al., 2005) with OL as the only available Fe source (and Si  
156 source for diatoms). For all experiments, cultures were sampled for a basic set of core  
157 biogeochemical and physiological parameters (Fu et al., 2005, 2008; Tovar-Sanchez et al., 2003;  
158 Paasche et al., 1996). This approach allowed us to compare phytoplankton taxon-specific  
159 responses, including: **1)** physiological impacts at extremely high OL concentrations, **2)**  
160 physiological thresholds and dose responses across a range of increasing concentrations of OL,  
161 and **3)** individual effects of specific OL constituents.

162

## 163 **Materials and Methods**

164

### 165 *Culture growth conditions and experimental set up*

166

167 Six species of phytoplankton were used in these experiments, including: the planktonic diatom  
168 *Ditylum brightwellii* (centric, planktonic, isolated by T. Ryneerson from Narragansett Bay,  
169 Rhode Island, USA) and the benthic diatom *Nitzschia punctata* (CCMP 561, isolated from tidal  
170 mud near San Diego, North Pacific Ocean), a coccolithophore, *Emiliana huxleyi* (CCMP 371, a  
171 North Atlantic isolate), a picoplanktonic cyanobacterium *Synechococcus sp.* (strain XM-24,  
172 isolated by J. Zheng from Xiamen estuary, the South China Sea, PRC, belonging to clade CB5,  
173 subcluster 5.2), and two marine dinitrogen (N<sub>2</sub>) fixing cyanobacteria, *Trichodesmium erythraeum*  
174 (strain IMS 101, from the Gulf Stream, Northwest Atlantic Ocean) and *Crocospaera watsonii*  
175 (WH 0005, from the North Pacific Ocean). Cultures were grown in 500 mL polycarbonate flasks  
176 at 28<sup>o</sup>C for the three cyanobacteria, and 20<sup>o</sup>C for the diatoms and *Emiliana huxleyi*. Cool-white  
177 fluorescent light was supplied following a 12:12 light:dark cycle at an irradiance level of 150  
178 μEm<sup>-2</sup>s<sup>-1</sup>. Stock cultures were grown in natural offshore seawater collected with trace metal clean  
179 methods (John et al., 2022), which was used to make modified Aquil Control Medium (ACM).  
180 The positive control ACM contained replete levels of nutrients and trace metals (i.e., 4 μM  
181 phosphate (PO<sub>4</sub><sup>3-</sup>), 60 μM nitrate (NO<sub>3</sub><sup>-</sup>), 250 nM Fe, 50 nM Co, no Cr or Ni, (Sunda et al.,  
182 2005)), and 60 μM silicate (SiO<sub>3</sub><sup>2-</sup>) was added to the ACM medium for culturing the two diatoms  
183 only.

184 For experiments, cultures were inoculated into the three Olivine Leachate (OL) treatments  
185 described below, with the addition of 4 μM phosphate (PO<sub>4</sub><sup>3-</sup>) and 60 μM nitrate (NO<sub>3</sub><sup>-</sup>). There  
186 was no nitrogen (N) added into the ACM or OL medium for the N<sub>2</sub> fixers. Iron, Cobalt, Nickel  
187 (Fe, Co and Ni) and silicate (SiOH<sub>4</sub>) were not added to the OL medium, except as components of  
188 the olivine leachate (see below). The background nutrient concentrations in the collected natural

189 seawater were  $1\mu\text{M NO}_3^-$ ,  $0.1\mu\text{M PO}_4^{3-}$  and  $3\mu\text{M SiOH}_4$ . Dissolved trace metals were not  
 190 measured, but surface concentrations are typically very low (1nM Fe or less, (John et al., 2012))  
 191 at the SPOT time series site where the seawater was cleanly collected, relative to amounts added  
 192 to the ACM and to the OL (**Table 1**) for phytoplankton culturing.

193  
 194 *Synthetic olivine leachate preparation*

195  
 196 To simulate acute exposure of phytoplankton to elevated levels of olivine dissolution products in  
 197 seawater, we prepared an artificial concentrated OL stock solution based on elemental analyses  
 198 of commercial ground olivine rock (Sibelco. (2022) Technical Data - Olivine Refractory Grade  
 199 Fine. Antwerp, Belgium). For experimental exposures, this concentrated OL stock was added to  
 200 seawater growth medium to yield the final concentrations shown in **Table 1**, which will be  
 201 referred to throughout as a “100%” concentration of OL. Experiments examining biological  
 202 effects across a dilution range (0-100%) used correspondingly lower additions of the  
 203 concentrated stock.

204  
 205 **Table 1.** Concentrations of added ions or compounds in serial dilutions of synthetic olivine  
 206 leachate (OL, 0% to 100%) used in the phytoplankton growth experiments; and concentrations of  
 207 components in the three concentrated stocks used to prepare experimental medium (1mL/L  
 208 added for 100% OL). Stock C was prepared in 10 nM HCl to keep the trace metals in solution  
 209 until addition.

	OL Added	Mg <sup>2+</sup> ( $\mu\text{M}$ )	SiOH <sub>4</sub> ( $\mu\text{M}$ )	OH <sup>-</sup> ( $\mu\text{M}$ )	Fe(II) ( $\mu\text{M}$ )	Ni(II) ( $\mu\text{M}$ )	Cr(VI) ( $\mu\text{M}$ )	Co(II) ( $\mu\text{M}$ )
Concentration added to growth medium	100%	44.9	25	100	3.36	0.13	0.12	0.006
	80%	35.9	20	80	2.7	0.10	0.10	0.005
	50%	22.5	12.3	50	1.7	0.07	0.06	0.003
	30%	13.5	7.5	30	1.0	0.04	0.04	0.002
	10%	4.5	2.5	10	0.34	0.01	0.01	0.001
	0%	0	0	0	0	0	0	0
Concentrated stock solutions (mM)		MgCl <sub>2</sub>	NaSiO <sub>2</sub>	NaOH	FeCl <sub>2</sub>	NiCl <sub>2</sub>	K <sub>2</sub> CrO <sub>4</sub>	CoCl <sub>2</sub>
Stock A		44.9						
Stock B			25	100				
Stock C					3.36	0.13	0.12	0.006

210  
 211 *Experimental methods*

212  
 213 Semi-continuous culturing methods were used to achieve nearly steady-state growth. Cultures  
 214 were diluted with fresh medium every 2 or 3 days, using in vivo fluorescence as a real time  
 215 biomass indicator. Dilutions were calculated to bring the cultures back down to the biomass

216 levels that were recorded after the previous day's dilution. In this way, cultures were allowed to  
217 determine their own growth rates under each set of experimental conditions, without ever nearing  
218 stationary phase, significantly depleting nutrients or self-shading (Fu et al., 2022). For all  
219 experiments, cultures were sampled for a basic set of core biomass and physiological parameters,  
220 including cell counts, CO<sub>2</sub> fixation, particulate organic carbon (POC), particulate organic  
221 nitrogen (PON), particulate organic phosphorus (POP) and biogenic silica (BSi, diatoms only)  
222 once steady-state growth was obtained for each growth condition (typically after 8–10  
223 generations). Steady-state growth status was defined as no significant difference in cell- or in  
224 vivo-specific growth rates for at least 3 consecutive transfers.

225

226 There were four sets of experiments in this project:

227

228 *1) Acute responses to elevated olivine leachate levels.* The goal of this set of experiments was to  
229 investigate the responses of the diatoms *Nitzschia* and *Ditylum* to relatively high concentrations  
230 of olivine leachate, in order to determine acute exposure responses. To see if the leachate may  
231 have a positive or negative effect on their physiology, they were compared to their respective  
232 control cultures. There were a total of three treatments consisting of: OL (100%), ACM, and  
233 ACM with low Fe/Si (with 2 nM Fe EDTA added, and no added SiOH<sub>4</sub>).

234

235 *2) Responses to a broad range of olivine leachate levels.* In these experiments, *Synechococcus*,  
236 *Crocospaera*, *Ditylum*, and *Emiliania huxleyi* were grown in culture medium across a series of  
237 OL dilutions (Table 1) to determine their responses across a range of leachate concentrations,  
238 from high to very low-level exposures.

239

240 *3) Fe bioavailability and Cr toxicity from olivine leachate to N<sub>2</sub>-fixing cyanobacteria.* The goal  
241 of this set of experiments was to investigate OL-derived Fe bioavailability to N<sub>2</sub>-fixing  
242 cyanobacteria, *Trichodesmium* and *Crocospaera*. An additional experiment was conducted to  
243 investigate potential Cr(VI) toxicity.

244

245 *4) Two species co-culture competition experiments during olivine leachate exposure.* In order to  
246 test how OL may affect co-existence and competition between the diatom *Ditylum* and the  
247 coccolithophore *Emiliania huxleyi*, a simple batch co-culture competition experiment was carried  
248 out in which the 2 species were inoculated at a 1:1 ratio (based on equivalent levels of cellular  
249 Chlorophyll a due to the large differences in their cell sizes) into 100% OL and regular ACM,  
250 and grown for 10 days until early stationary phase. In vivo fluorescence and cell counts were  
251 monitored daily. Relative abundance and growth rates of the two species were determined based  
252 on microscopic cell counts during the exponential growth phase of the mixed cultures. Biogenic  
253 silica (BSi, an indicator of diatom abundance) and particulate inorganic carbon (PIC or calcite,  
254 an indicator of coccolithophore abundance) were collected every other day in order to further  
255 determine how these two species responded to co-culture with and without leachate additions.

256  
257  
258  
259  
260  
261  
262  
263  
264  
265  
266  
267  
268  
269  
270  
271  
272  
273  
274  
275  
276  
277  
278  
279  
280  
281  
282  
283  
284  
285  
286  
287  
288  
289  
290  
291

*Analytical methods*

Determination of growth rates and chlorophyll a Growth rates were determined based on changes in chlorophyll a. For chlorophyll a determination, subsamples of 30 ml from each triplicate bottle were GF/F filtered, extracted in 6 ml of 90% acetone, stored overnight in the dark at  $-20^{\circ}\text{C}$ , and chlorophyll a concentrations were measured fluorometrically using a Turner 10-AU fluorometer (Welschmeyer, 1994). Specific growth rates were determined using the equation:

$$\mu = \frac{\ln\left(\frac{N_{T_{final}}}{N_{T_{initial}}}\right)}{T_{final} - T_{initial}}$$

where  $\mu$  is the specific growth rate (per day) and  $N$  is the chlorophyll a concentration at  $T_{initial}$  and  $T_{final}$  (Kling et al., 2021).

Particulate C, N, P and Si. Particulate organic carbon and nitrogen (CHN) samples from all experiments were filtered (pre-combusted GF/F) and frozen for analysis using a Costech Elemental Analyzer (Hutchins et al., 2007). Samples for biogenic silica (BSi) were filtered onto 25 mm diameter, 0.6  $\mu\text{m}$  pore size polycarbonate filters (Pall Life Sciences), and analyzed according to (Brzezinski, 1985). POP (particulate organic phosphorus) samples were collected onto pre-combusted 25 mm GF/F filters and analyzed as in Fu et al. 2005 (Fu et al., 2005).

Primary productivity. For all species other than the coccolithophore (see below), primary production was measured in triplicate using 24h incubations (approximating net PP) with  $\text{H}^{14}\text{CO}_3$  under the appropriate experimental growth conditions for each treatment (Fu et al., 2008).  $\text{CO}_2$  fixation rates were calculated using measured final experimental DIC concentrations and biomass. All samples for primary production were counted using a Wallac System 1400 liquid scintillation counter.

Photosynthetic and calcification rates of *Emiliana huxleyi*. For the coccolithophore, two 40 mL subsamples from each triplicate bottle were spiked with 0.5  $\mu\text{Ci}$   $\text{NaH}^{14}\text{CO}_3$ . One subsample was incubated in the light and the other in the dark for 24 h. Then two sets of 20 mL aliquots from each sub-sample were filtered onto Whatman GF/F filters. The filters for photosynthetic rate determination were fumed with saturated HCl before adding scintillation cocktail fluid. Photosynthetic rate and calcification rate were calculated as described in Paasche et al. 1996 (Paasche et al., 1996).



292 Nitrogen fixation rates of *Crocospaera watsonii*. In order to estimate the N<sub>2</sub> fixation rates of  
293 *Crocospaera*, initial and final particulate organic nitrogen samples (50mL) were collected on  
294 combusted GF/F filters over a 24 hr incubation. The PON specific N<sub>2</sub> rates were calculated using  
295 the following equation:

$$N_{fix} = \frac{\left( \frac{PON_{T_{final}} - PON_{T_{initial}}}{PON_{T_{initial}}} \right)}{T_{final} - T_{initial}}$$

296  
297  
298  
299 where Nfix is the N specific N<sub>2</sub> fixation rates (day<sup>-1</sup>) and PON is the particulate organic nitrogen  
300 at Tinitial and Tfinal as measured using an elemental analyzer (Costech Analytical  
301 Technologies) (Fu et al., 2014)  
302

303 Fe quota. Intracellular Fe content was determined by filtering culture samples onto acid-washed  
304 0.2-µm polycarbonate filters (Millipore), and rinsing with oxalate reagent to remove extracellular  
305 trace metals (Tovar-Sanchez et al., 2003). Fe was determined with a magnetic sector-field high-  
306 resolution inductively coupled plasma mass spectrometer (ICPMS) (Element 2, Thermo) (Jiang  
307 et al., 2018; John et al., 2022).  
308

309 Statistical methods. A one-way ANOVA analysis of variance was used to analyze differences  
310 between treatments using Prism 8. Differences between treatments were considered significant at  
311 p<0.05. Post-hoc comparisons were conducted using the Tukey's multiple comparison test to  
312 determine any pairwise differences. Equality of variance was verified for all data using F tests,  
313 and the Shapiro Wilk test was used to test for significant departures from normality, which was  
314 not the case for any of our data sets. For experiments with only one or two OL treatments and  
315 the ACM control, graphs are presented with each treatment marked with a letter denoting  
316 significant differences at the p < 0.05 level from each of the other treatments. For experiments  
317 such as OL dilution series with many treatments (7 in this case), clear visualization of differences  
318 with all other treatments using letters is not feasible. For these experiments, significant  
319 differences in the OL treatments relative to the ACM positive control are indicated by asterisks  
320 (\* = p < 0.05; \*\* = p < 0.01; \*\*\* = p < 0.001; \*\*\*\* = p < 0.0001). For all experiments, actual p  
321 values are given in the text.  
322  
323

## 324 Results

### 326 *Diatoms*

327 We hypothesized that the diatoms might benefit from the OL products Si and Fe, as they  
328 are both required for growth and can be limiting for this group (Tréguer et al., 2018). Hence, we  
329 grew the benthic diatom *Nitzschia* across three treatments: 100% OL alone, Aquil control  
330 medium (ACM), and ACM but with low, limiting Si and Fe concentrations (ACM-low-SF).  
331 *Nitzschia* grew and fixed carbon just as well in the 100% OL as the ACM (p=0.35; p=0.21),

332 while showing reduced rates in the ACM-low-SF treatment ( $p=0.02$ ;  $p<0.0001$ ; **Fig. 1A, B**).  
 333 Likewise, the particulate Si:C ratios demonstrated 100% OL to be just as good a source of Si to  
 334 *Nitzschia* as the ACM ( $p=0.98$ ), and considerably better than the ACM-low-SF ( $p=0.0012$ ; **Fig.**

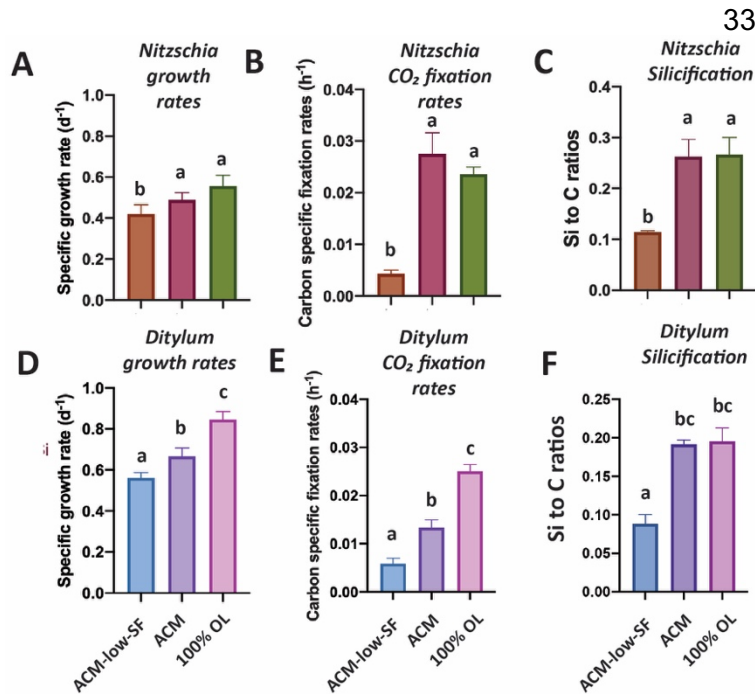


**Fig 1. Effects of olivine leachate versus culture medium controls on growth and physiology of a benthic and pelagic diatom. A) and D) are Cell-specific growth rates (d<sup>-1</sup>), B) and E) are Carbon-specific fixation rates (hr<sup>-1</sup>) and C) and F) are Si:C ratios (mol:mol) for the diatoms *Nitzschia punctata* (benthic) and *Ditylum brightwellii* (pelagic), respectively. Abbreviations: OL is 100% olivine leachate, ACM is positive control Aquil medium, ACM-low-SF is positive control Aquil medium with lowered Si and Fe concentrations. Y-axis values represent the means, and error bars are the standard deviations of biological triplicate cultures for each treatment. Different letters indicate significant differences at the  $p < 0.05$  level.**

**1C).** Growth and CO<sub>2</sub> fixation rates of the planktonic diatom *Ditylum* were significantly higher in the 100% OL treatment compared to either the ACM ( $p=0.002$ ;  $p=0.0001$ ) or ACM-low-Si/Fe treatments ( $p=0.0002$ ;  $p<0.0001$ ; **Fig. 1D, E**), while Si:C ratios were the same ( $p=0.93$ ; **Fig. 1F**). When *Ditylum* was grown across a range of OL concentrations (i.e., a dilution series from 0% to 100% additions, where 100% corresponds to the 100% OL treatment), we observed increasing growth and CO<sub>2</sub> fixation rates with increasing OL concentrations, with maximum rates observed at and above 50% of the original OL that were not significantly different from those in the ACM control ( $p=0.06$ , 0.33, 0.99, **Fig. 2A, B**). *Ditylum* particulate Si:C ratios also reached levels not significantly different to those seen in the

363 ACM medium in the 100% additions ( $p=0.07$ , **Fig. 2C**). Likewise, *Ditylum* cellular Fe:P ratios  
 364 measured by ICP-MS were not significantly different between 100% OL and ACM treatments,  
 365 suggesting the diatom could access the same amount of Fe from the precipitated Fe(III) in the  
 366 OL as from the soluble (EDTA-chelated) Fe(III) in the ACM culture medium ( $p=0.56$ ; **Supp.**  
 367 **Fig 1A**). These data demonstrate that even at extremely high concentrations, olivine dissolution  
 368 products including trace metals were not toxic to these diatoms, but instead may provide sources  
 369 of the essential nutrients iron and silicate to support their growth in nutrient replete conditions.

370  
 371 *Coccolithophores*

372 It has been hypothesized that calcifying coccolithophores may benefit from an increase in  
 373 alkalinity from olivine dissolution (Bach et al., 2019). In the OL dilution series, maximum  
 374 growth rates for the coccolithophore *Emiliana* equivalent to those recorded in the ACM positive  
 375 control medium were achieved at all added OL concentrations from 10% to 100% (p=0.36,0.92,

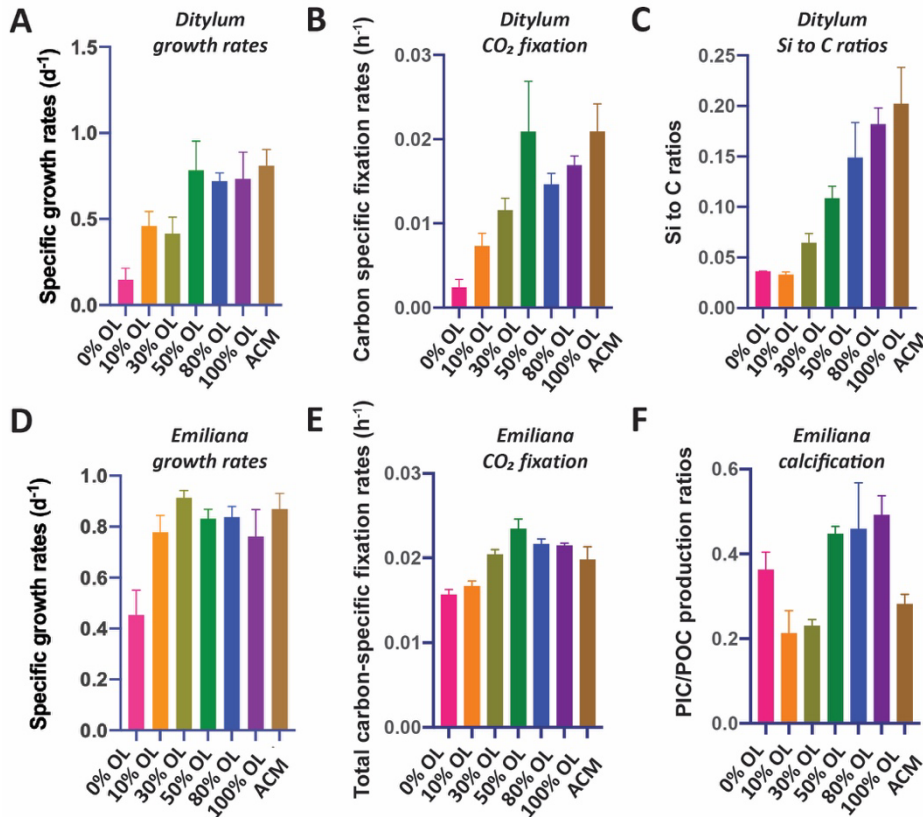


**Fig 2. Effects of a dilution series of olivine leachate on growth and physiology of a marine diatom and coccolithophore.** The diatom *Ditylum brightwellii* and the coccolithophore *Emiliana huxleyi* were grown across a range of dilutions of the olivine leachate (OL, 0-100%), and in the positive control medium (ACM). Shown are: **A)** Cell-specific growth rates (d<sup>-1</sup>), **B)** Carbon-specific fixation rates (hr<sup>-1</sup>) and **C)** Si:C ratios (mol Silicon: mol Carbon) of *Ditylum brightwellii*, and: **D)** Cell-specific growth rates (d<sup>-1</sup>), **E)** Carbon-specific fixation rates (hr<sup>-1</sup>), and **F)** PIC/POC production ratios (calcification production rate/organic carbon fixation rate, unitless) of *Emiliana huxleyi* in the same OL and ACM treatments. Y-axis values represent the means and error bars are the standard deviations of biological triplicate cultures for each treatment. Relative to the ACM positive control, significant differences in OL treatments are indicated by \* = p < 0.05; \*\* = p < 0.01; \*\*\* = p < 0.001; \*\*\*\* = p < 0.0001.

407 **Fig. 2E).**

408 **Particulate inorganic carbon to particulate organic carbon production**  
 409 **ratios) were significantly higher at OL levels of 50-100% than in the ACM positive controls**  
 410 **(p=0.009, 0.005, 0.001, Fig. 2F), possibly due to enhanced alkalinity in the high OL**  
 411 **concentration treatments. PIC:POC production ratios were elevated in the 0% OL**

412 relative to those in the 10% and 30% OL treatments due to CO<sub>2</sub> fixation rates being reduced  
 413 more than PIC fixation rates in this treatment, but in none of these treatments was this parameter  
 414 significantly different from the ACM control (p=0.30,0.45,0.70, **Fig. 2F**).

415 An independent set of basic two-treatment experiments with the coccolithophore (ACM  
 416 versus 100% OL, **Supp. Fig 2**) supported the results of the dilution series experiments shown in  
 417 **Fig. 2**. *Emiliana* specific growth rates were slightly higher in the OL than in the ACM (p =  
 418 0.05), while cellular particulate inorganic:particulate organic carbon ratios (PIC:POC, mol:mol)  
 419 were not significantly different in the two treatments (p= 0.08, **Supp. Fig. 2A**). Likewise, both  
 420 POC-specific fixation rates (p=0.04; TC h<sup>-1</sup>) and PIC:POC production ratios were slightly higher

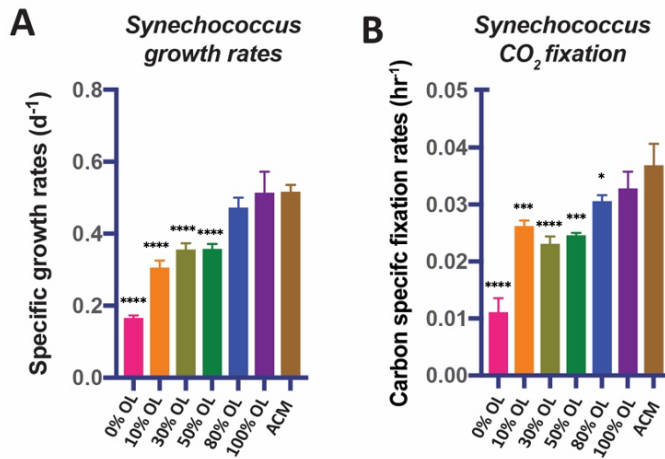


**Fig 3. Effects of a dilution series of olivine leachate on growth and CO<sub>2</sub> fixation of a marine cyanobacterium.** The unicellular picocyanobacterium *Synechococcus* sp. was grown across a range of dilutions of the olivine leachate (OL, 0-100%), and in the positive control medium (ACM). Shown are: **A**) Cell-specific growth rates (d<sup>-1</sup>) and **B**) Carbon-specific fixation rates (hr<sup>-1</sup>). Values represent the means and error bars are the standard deviations of triplicate cultures for each treatment. Relative to the ACM positive control, significant differences in OL treatments are indicated by \* = p < 0.05; \*\* = p < 0.01; \*\*\* = p < 0.001; \*\*\*\* = p < 0.0001.

443

444 and CO<sub>2</sub> fixation rates (**Fig. 3B**) across the range of OL levels, similar to those of the eukaryotic  
 445 algae. Both growth rates and carbon fixation rates were the same in the 100% OL treatment as in  
 446 the ACM positive control treatment (p=0.94; p=0.46). ICP-MS measurements of *Synechococcus*  
 447 cellular Fe:P ratios across a range of OL levels (0-100%) showed that this isolate accumulated  
 448 much less Fe in the 0% OL than in the ACM treatment (p=0.02), but in all treatments with added  
 449 OL, Fe:P ratios were the same as (10%. p=0.99, 30% 0.30, 50% 0.13, 100% 0.17) or higher than  
 450 (80% p=0.01) than the ACM values (**Supp. Fig. 1B**). As with the eukaryotic phytoplankton

in the OL than in the ACM  
 treatments (p=0.05, **Supp. Fig. 2B**).  
 Like the diatoms, these data  
 demonstrate that olivine dissolution  
 products are also not toxic to this  
 common coccolithophore species,  
 and that enhanced alkalinity may  
 support marginally higher growth  
 rates under nutrient replete  
 conditions.

### Cyanobacteria

Like diatoms and  
 coccolithophores, cyanobacteria  
 could benefit from olivine  
 dissolution due to their relatively  
 high Fe (Hutchins and Boyd, 2016)  
 and Ni requirements (Dupont et al.,  
 2008). The OL dilution series  
 experiments using the widely  
 distributed picocyanobacterium  
*Synechococcus* showed positive  
 responses in growth rates (**Fig. 3A**)

451 tested, the synthetic OL provided a good source of Fe to support the growth of the  
452 picocyanobacterium.

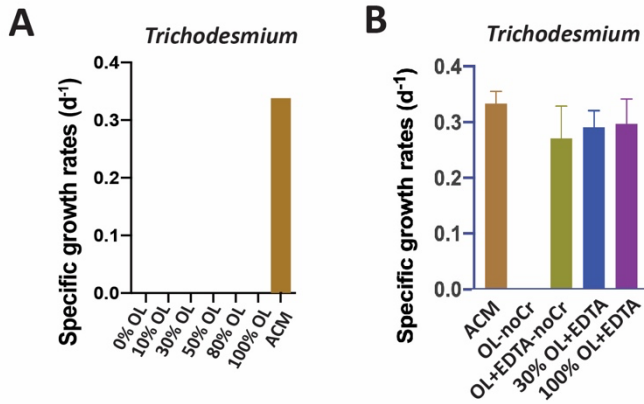


**Fig 4. Effects of olivine leachate versus culture medium controls on growth of a colonial marine N<sub>2</sub>-fixing cyanobacterium.** Shown are **A**) Cell-specific growth rates (d<sup>-1</sup>) of the colonial cyanobacterium *Trichodesmium erythraeum* across a range of dilutions of the olivine leachate (OL, 0-100%) and in the positive control medium (ACM), and **B**) Cell-specific growth rates (d<sup>-1</sup>) of *Trichodesmium* in two concentrations of OL (30% and 100%) with the synthetic metal chelator EDTA, and in OL without Cr or EDTA, and in OL without Cr but plus EDTA, all versus ACM. Unless growth rates were zero, relative to the ACM positive control, significant differences in OL treatments are indicated by \* = p < 0.05; \*\* = p < 0.01; \*\*\* = p < 0.001; \*\*\*\* = p < 0.0001.

In striking contrast to the eukaryotic algae and the non-diazotrophic (i.e., non-N<sub>2</sub>-fixing) picocyanobacterium *Synechococcus*, the N<sub>2</sub>-fixing cyanobacterium *Trichodesmium* could not grow at any concentration of OL tested (**Fig. 4A**). One possible explanation for this lack of growth is toxic effects by one of the trace metal components of the OL. We hypothesized that added levels of Ni and Co are unlikely to be toxic, as these nutrient metals have been found to be relatively non-toxic to many phytoplankton at similar environmental concentrations (Guo et al., 2022; Karthikeyan et al., 2019; Panneerselvam et al., 2018). Hence, we hypothesized that Cr toxicity should be considered as a likely possible scenario (Frey et al., 1983; Kiran et al., 2016). Another possibility is that *Trichodesmium* did not experience toxic effects but instead was unable to access Fe from OL. This N<sub>2</sub>-fixer requires

476 more Fe than virtually any other phytoplankton species (Hutchins and Sañudo-Wilhelmy, 2021),  
477 and the OL was the only source of Fe provided in our experiments. Fe(II) released into seawater  
478 from olivine dissolution likely quickly oxidizes to Fe(III), which then precipitates and becomes  
479 insoluble at the elevated concentrations in our OL (Manck et al., 2022). This could render it  
480 biologically unavailable to the cellular Fe uptake systems of some species. We deliberately  
481 designed our OL to replicate this oxidation/precipitation process, and as expected observed  
482 visible reddish-brown amorphous colloidal Fe precipitates on the bottom of the growth flasks for  
483 all synthetic OL treatments. It is possible that other metals including Ni may have co-precipitated  
484 with the iron, as has been documented in other aquatic systems (Laxen 1985). If so, this would  
485 lower dissolved Ni levels, a process that could also occur during olivine deployments in the  
486 ocean.

487 Accordingly, we designed another set of experiments to test for both lack of Fe  
488 bioavailability and specific sensitivity to Cr, as has been done in previous cyanobacterial studies  
489 (Kiran et al., 2016). To do this, we formulated several variants of the olivine leachate: 1) normal  
490 OL (100% concentration), 2) OL (100% concentration) with a synthetic ligand (EDTA) that

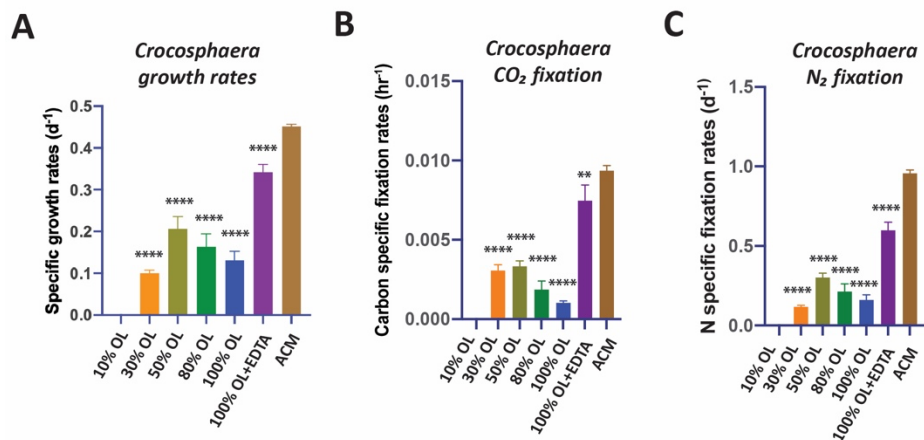


**Fig 5. Effects of olivine leachate dilution series versus culture medium controls on the physiology of a unicellular marine N<sub>2</sub>-fixing cyanobacterium.**

A) Cell-specific growth rates (d<sup>-1</sup>), B) Carbon-specific fixation rates (hr<sup>-1</sup>), and C) N-specific fixation rates (day<sup>-1</sup>) of the unicellular cyanobacterium *Crocospaera watsonii* grown across a range of dilutions of the olivine leachate (OL, 0-100%), in 100% OL plus EDTA (OL+EDTA), and in the positive control medium (ACM). Values represent the means and error bars are the standard deviations of triplicate cultures for each treatment. Relative to the ACM positive control, significant differences in OL treatments are indicated by \* = p < 0.05; \*\* = p < 0.01; \*\*\* = p < 0.001; \*\*\*\* = p < 0.0001.

511

512 that the lack of growth observed in OL was not due to Cr toxicity. However, growth recovered to  
 513 the same levels as in the ACM in all three treatments where EDTA was added (30%OL+EDTA  
 514 p=0.62, 100%OL+EDTA p=0.84, 100%OL+EDTA-noCr p=0.30) to the leachate (Fig. 4B).  
 515 Together, these results suggest that poor bioavailability of the precipitated Fe(III) (and not Cr  
 516 toxicity) was the likely cause for *Trichodesmium*'s inability to grow in the unmodified OL.

517 OL also reduced the growth rates of the unicellular N<sub>2</sub>-fixing cyanobacterium  
 518 *Crocospaera*, although not to the same extent as for *Trichodesmium*, which didn't grow at all  
 519 without the addition of EDTA. *Crocospaera* exhibited no growth at 0% OL, likely due to  
 520 severe Fe limitation. From 10% to 100% OL, growth rates were 22-44% of those in ACM  
 521 (p<0.001), and growth partially recovered in 100% OL+EDTA to 76% of rates in ACM  
 522 (p<0.0001, Fig. 5A). Results were very similar for CO<sub>2</sub> fixation rates and N<sub>2</sub>-fixation rates in  
 523 OL, which were severely reduced by 64-100% (carbon fixation, p<0.0001) and 69-88% (N<sub>2</sub>  
 524 fixation, p<0.0001) relative to ACM in all OL treatments, but reached maximum values of 80%  
 525 (p=0.002) and 63% (p<0.0001) of ACM treatment rates, respectively, when EDTA was added to  
 526 the OL (Fig. 5B,C). This suggests that oxidized Fe from OL was not effectively utilized to  
 527 support growth for either of the two N<sub>2</sub>-fixing cyanobacteria tested, in contrast to the diatoms,  
 528 coccolithophores, and *Synechococcus*. Their growth recovery after EDTA additions indicates  
 529 that the other trace metals Cr, Ni, and Co in the olivine leachate were likely not toxic, even at  
 530 extremely high concentrations. Interestingly, unlike *Trichodesmium* which could not grow at all

solubilizes Fe(III),  
 and thus makes it  
 broadly  
 bioavailable  
 (OL+EDTA), 3)  
 OL (100%  
 concentration) but  
 with no Cr (OL-  
 noCr), 4) and OL  
 (100%  
 concentration) but  
 with no Cr and with  
 EDTA  
 (OL+EDTA-noCr)  
 (Fig. 4B).  
*Trichodesmium* also  
 could not grow in  
 the OL medium  
 without added Cr  
 (OL-noCR, Fig.  
 4B), demonstrating

531 on OL alone but recovered fully upon EDTA additions, *Crocospaera* could still grow at lower  
532 rates on OL but could not grow as fast upon EDTA additions as in ACM. Future experiments are  
533 needed to understand these differences in species-specific responses between these two N<sub>2</sub>-  
534 fixers. Taken together, these data suggest that when olivine dissolves in seawater, it is unlikely to  
535 provide a readily bioavailable Fe source to diazotrophic cyanobacteria, although this does not  
536 preclude them obtaining Fe from their usual natural sources such as other sediments, rivers, dust  
537 inputs etc. Thus, it seems likely that olivine may have negligible or no effect (positive or  
538 negative) on the physiology of these cyanobacteria, although further work will be needed to put  
539 these results into a more realistic ecological context to understand the full responses of N<sub>2</sub> fixing  
540 cyanobacteria to olivine dissolution.

541

#### 542 *Diatom/Coccolithophore Competitive Co-culture*

543 Results of the co-culture, or competition, experiment with the diatom *Ditylum*  
544 *brightwellii* and the coccolithophore *Emiliania huxleyi* are shown in **Fig. 6**. Unlike the semi-  
545 continuous experiments shown in the previous figures, this experiment used closed-system  
546 “batch” culturing methods in order to assess and compare effects on relative biomass  
547 accumulation by each species over time. OL (100% concentration) supported growth of both the  
548 diatom (**Fig. 6A**) and the coccolithophore (**Fig. 6B**) in mixed culture, and biomass was very  
549 similar for both species between the OL and ACM treatments throughout most of the  
550 experiment. However, cell yields were higher in the ACM at the final timepoint for the diatom ( $p$   
551 = 0.009, **Fig. 6A**). Final cell counts were also higher in the ACM for the coccolithophore, but  
552 this difference was not significant ( $p = 0.31$ ; **Fig. 6B**). Similar trends were observed when diatom  
553 biomass was estimated as biogenic silica (BSi, **Fig. 6C**,  $p = 0.002$ ) and when coccolithophore  
554 biomass was assessed as calcite or particulate inorganic carbon (PIC, **Fig. 6D**,  $p = 0.04$ ). For the  
555 diatom, OL supported growth rates similar to those in the ACM treatment during the first half of  
556 the experiment (**Fig. 6A,C; Supp. Fig. 3A**). Growth rates were also similar in the OL and ACM  
557 mediums for the coccolithophore (**Fig. 6B,D; Supp. Fig. 3B**). Hence, both phytoplankton  
558 species were able to grow similarly well in co-culture, where neither exhibited any strong  
559 competitive advantage over the other.

560

561

562

563

564

565

566

567

568

569

570

571 **Discussion**

572

573

574

575

In general, we observed no toxic effects from our simulated olivine dissolution products even at extremely high concentrations across all the phytoplankton species tested, consistent with other recent observations examining OAE scenarios (Gately et al., 2023) and trace metals (Guo

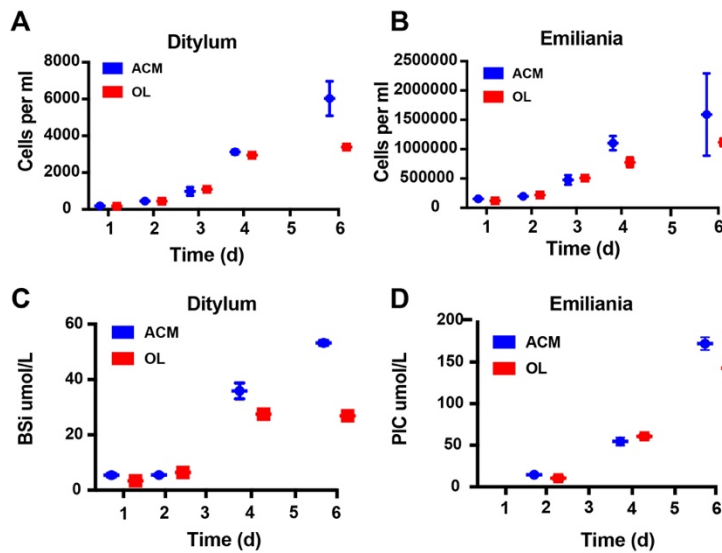


**Fig. 6. Effects of olivine leachate versus culture medium controls on growth competition and biomineralization during co-culture of a diatom and a coccolithophore.** Shown are 5-day growth curves (cells  $\text{mL}^{-1}$ ) for **A**) the diatom *Ditylum brightwellii* and **B**) the coccolithophore *Emiliana huxleyi* in mixed cultures grown in olivine leachate (OL, red symbols) and positive control medium (ACM, blue symbols). Also shown are **C**) Biogenic silica (BSi,  $\mu\text{mol L}^{-1}$ ), a proxy for diatom biomass, and **D**) Calcite or particulate inorganic carbon (PIC,  $\mu\text{mol L}^{-1}$ ), a proxy for coccolithophore biomass, in the OL and ACM treatments in the same growth competition experiment. Values represent the means and error bars are the standard deviations of triplicate cultures for each treatment.

601

602

603

604

605

606

607

608

609

relative to the total dissolved Ni pool. Although broad negative effects of enhanced Ni concentrations were not observed across taxa, Guo observed some species-specific responses across variations in (0-100  $\mu\text{M}$ ) EDTA and Ni (0-50  $\mu\text{M}$ ) concentrations, indicating that specific phytoplankton groups are impacted differently depending on the chemical species in the total dissolved Ni pools and/or the concentration and type of organic ligands in seawater. Our results are generally consistent with their overall findings, as the phytoplankton groups tested here did not exhibit negative effects upon elevated exposure to Ni with (e.g., ACM) and without added EDTA (e.g., OL), suggesting that Ni was not toxic irrespective of the concentration of different Ni species in the dissolved pool or that of the  $\text{Ni}^{2+}$  ion. However, our experiments were not

et al., 2022). Guo et al. (2022)

particularly focused on exposing

11 phytoplankton groups to

elevated Ni concentrations and did

not observe strong effects across

these taxa. Although it is

unknown what chemical species

of dissolved Ni primarily

influence phytoplankton

physiology, most studies indicate

that phytoplankton primarily

interact with free  $\text{Ni}^{2+}$  ions but are

not particularly sensitive to the

total dissolved Ni concentration

(Guo et al., 2022). Guo et al.

(2022) and our study used the

same Ni-containing compound,

$\text{NiCl}_2$ , as a source of  $\text{Ni}^{2+}$ . Guo et

al. also used the same base Aquil

control medium as our ACM.

ACM contains EDTA that binds

with metal ions like Ni to improve

their dissolution, which

subsequently lowers the free Ni

ion concentrations (e.g.,  $\text{Ni}^{2+}$ )



610 designed to test for taxon-specific differences in responses to specific Ni species or variations in  
611 EDTA concentrations.

612 The two diatoms were able to use synthetic OL-derived Si and Fe to support near-  
613 maximum growth rates and carbon fixation rates, as well as robust silica frustule development  
614 (as assessed by cellular Si:C ratios); both of these nutrients can frequently limit diatom growth in  
615 various parts of the ocean (Tréguer et al., 2018; Hutchins and Boyd, 2016). OL-derived  
616 alkalinity and iron increases also supported growth of the tested coccolithophore, consistent with  
617 previous observations showing increases in red algae calcification (Gore et al., 2019) and net reef  
618 calcification calcifying corals (Albright et al., 2016) in response to OAE. Similarly, a  
619 representative of the globally distributed, picocyanobacterium *Synechococcus* increased its  
620 growth and carbon fixation rates as OL concentrations increased. Although OL could not support  
621 *Trichodesmium* and *Crocospaera* growth due to their inability to use Fe(III), olivine dissolution  
622 products were not observed to be toxic. Their inability to use Fe(III) is a neutral effect due to  
623 other sources of bioavailable Fe in the water column (Hutchins and Boyd, 2016).

624 Thus, these results using 6 model species suggest that many phytoplankton species may  
625 not be negatively impacted by even high levels of elements derived from olivine dissolution, and  
626 that some olivine dissolution products may support their growth, primary productivity, and  
627 biomineralization when OL is available at high enough concentrations in certain environmental  
628 conditions. For example, it is important to note that potential growth benefits to phytoplankton *in*  
629 *situ* will also depend on ambient concentrations of other important nutrients, such as nitrogen (N)  
630 and phosphorus (P). Our cultures contained an abundance of other required nutrients, thus  
631 enabling phytoplankton to take advantage of dissolution products for growth (e.g., Si, Fe,  
632 alkalinity). However, if nutrients like N and P are primarily limiting in natural environments,  
633 then olivine dissolution products are not expected to have any growth effect. In addition, these  
634 cultures represent closed systems that do not allow olivine products to be diluted with fresh  
635 seawater. In natural settings, advection in both sediment porewaters (Reimers et al., 2004) and  
636 the water column (He and Tyka, 2022) will lead to short residence times, thereby rapidly diluting  
637 olivine dissolution products. Hence, these physical dynamics will prevent high concentrations of  
638 olivine dissolution products from accumulating in seawater in coastal systems. Thus, even the  
639 most dilute leachate treatment in this study is likely more concentrated than the anticipated  
640 concentrations of olivine dissolution products expected under field conditions. It is important to  
641 note though that our experiments focused on physiological responses, while further work will be  
642 needed to explore the possibility of indirect effects on important ecological factors such as  
643 predation or competition. Further research will also be needed to test for direct and indirect  
644 effects using other species of phytoplankton not examined here and belonging to other important  
645 functional groups.

646 Bach et al. (2019) (Bach et al., 2019) hypothesized that under nutrient-limited conditions,  
647 silicate, iron and nickel releases from marine applications of silicate minerals like olivine might  
648 particularly benefit diatoms and cyanobacteria, as these groups have especially high  
649 requirements for one or more of these nutrients. Thus, they expected that olivine applications

650 might produce a “Greener” ocean. They also suggested that adding minerals derived from  
651  $\text{CaCO}_3^-$  (such as quicklime applications) would particularly favor coccolithophores, due to  
652 rapidly enhanced seawater alkalinity. This outcome would produce a “Whiter” ocean (the color  
653 of coccolithophore calcite). Although we did not test  $\text{CaCO}_3^-$  derivatives, our results with  
654 nutrient-replete synthetic OL seem to represent a “Green and White” ocean scenario, since in  
655 individual experiments diatoms, picocyanobacteria, and coccolithophores all responded  
656 positively to OL at the relatively elevated levels applied in our experiments. This conclusion is  
657 further supported by the results of our nutrient replete diatom/coccolithophore co-culture  
658 experiment, which showed that OL stimulated both species simultaneously rather than conferring  
659 a competitive advantage on one or the other. This suggests that in the ocean, competitive  
660 outcomes between diatoms and coccolithophores may not be affected by olivine dissolution  
661 under nutrient-replete conditions, although we did not test this under nutrient-limited conditions  
662 that are commonly encountered by phytoplankton in nature.

663 Iron in olivine minerals is present as reduced Fe(II), and we added it in this form to our  
664 synthetic OL. However, when Fe(II) dissolves in oxic seawater, it quickly (within minutes)  
665 oxidizes to highly insoluble Fe(III), which precipitates out as amorphous iron hydroxides  
666 (Millero et al., 1987). Clearly, in our experiments this oxidized particulate iron must have been  
667 available to the species that showed growth enhancement with OL, since no other iron source  
668 was provided in the seawater growth medium. In accordance with their well-studied reductive Fe  
669 uptake systems (Morrissey and Bowler, 2012), there is evidence that diatoms can access Fe to  
670 some degree from freshly precipitated amorphous colloidal Fe hydroxides (like those in our  
671 experiments), although the bioavailability of Fe precipitates declines quickly as the hydroxides  
672 age and acquire a more crystalline structure (Yoshida et al., 2006). Alternately, the precipitated  
673 Fe in our experiments could have become available to the phytoplankton ferric reductases via  
674 solubilization by siderophores produced by bacteria in our non-axenic cultures (Coale et al.,  
675 2019). In some cases diatoms, can also potentially take up Fe through endocytosis (Kazamia et  
676 al., 2018).

677 The responses of the two  $\text{N}_2$ -fixing cyanobacteria were in striking contrast to those of the  
678 other three phytoplankton groups tested. These diazotrophs were either unable to grow in our  
679 artificial OL at all (*Trichodesmium*), or could only grow to a very limited degree  
680 (*Crocospaera*). However, our results with experimental additions of the artificial iron chelator  
681 EDTA (ethylene diamine tetra acetic acid) suggest that other mechanisms may enable iron  
682 bioavailability. For example, previous research has suggested that *Trichodesmium* cannot  
683 directly access particulate Fe(III) forms, but likely relies on bacteria residing on and in natural  
684 colonies to produce siderophores, which then solubilize particulate Fe(III) sources and make  
685 them bioavailable (Rubin et al., 2011; Lee et al., 2018). Since cultured *Trichodesmium* such as  
686 ours typically do not produce colonies, but grow instead as individual filaments of cells, cultures  
687 of this diazotroph are likely deficient in many of these iron-acquiring microbial symbionts  
688 (Rubin et al., 2011). The iron uptake systems of *Crocospaera* have been less well-  
689 characterized, but like *Trichodesmium*, molecular studies suggest this unicellular diazotroph

690 lacks the genetic capacity to produce endogenous siderophores (Shi et al., 2010; Yang et al.,  
691 2022). Our results show that when we add the artificial iron chelator EDTA (which substitutes  
692 for ligands produced by the missing bacteria in cultures), the synthetic OL supports near-  
693 maximum growth of both diazotrophs. Thus, reduced growth rates of these cyanobacteria in OL  
694 without EDTA appear to be due to severe iron limitation, not toxicity of any OL component. In  
695 our experiments the cells were forced to grow on OL as a sole source of iron, but in coastal  
696 ecosystems where olivine deployments would occur, there are typically many other natural  
697 sources of iron to support algal growth (Capone and Hutchins, 2013; Hutchins and Boyd, 2016).  
698 In nature, *Trichodesmium* is also likely to occur mostly as colonies, and so may have access to  
699 additional siderophore-bound iron, including from both naturally occurring supplies as well as  
700 potentially from any oceanic olivine applications. Thus, changes in the iron nutritional status of  
701 N<sub>2</sub> fixers due to olivine additions in-situ may not occur in the real ocean.

702 While the reduced growth rates of the diazotrophs on our synthetic OL appears to be due  
703 to iron limitation, our experiments also shed light on potential effects of other trace metals  
704 present in the formulation. Of the metals found in our synthetic OL, Ni and Co are considered  
705 nutrient elements with relatively low toxicity; in fact, the concentrations added even in our  
706 maximum dosage experiments were well below those that have been reported to be toxic to  
707 phytoplankton (Karthikeyan et al., 2019; Vink and Knops, 2023). However, Cr has the potential  
708 to be biologically problematic. Cr(III) found in olivine is relatively insoluble, so in this form it is  
709 probably not a major source of exposure for planktonic organisms. However, if it oxidizes to  
710 Cr(VI), it becomes much more soluble, and thus more bioavailable and potentially toxic. Cr(III)  
711 oxidation is thermodynamically unfavorable, but can be facilitated by borate ions always present  
712 in seawater, or by the presence of biologically or photochemically-produced oxidants like H<sub>2</sub>O<sub>2</sub>  
713 (Pettine et al., 1991), and by naturally occurring manganese oxides (Weijden and Reith, 1982).  
714 For these reasons, following the principle of “worst case scenario”, we used a soluble Cr(VI) salt  
715 in our synthetic OL formulation. Despite this, we found that the presence or absence of the  
716 relatively elevated levels of dissolved Cr(VI) in our regular synthetic OL did not make any  
717 difference to the growth of *Trichodesmium* or the other tested phytoplankton species.  
718 Particularly, because synthetic OL stimulated near-maximum growth rates in the diatoms,  
719 coccolithophore and picocyanobacterium, we presume that the Cr(VI) additions did not  
720 adversely affect these groups either.

721 The goal of this work was to test both extreme levels and simultaneous exposure of  
722 multiple, biologically important olivine dissolution products that could influence microbial  
723 physiology in order to identify thresholds and response curves. Accordingly, our experiments  
724 focused on determining acute effects of high concentrations of olivine dissolution products. In  
725 general, they suggest that negative impacts may be few even for large olivine deployments, given  
726 the high concentrations of tested olivine dissolution products. Because these microplankton serve  
727 as important links to higher trophic levels, these data suggest minimal long-term impacts from  
728 olivine dissolution on ecosystem services. Future research directions may include longer term  
729 experiments with prokaryotes and natural microbial communities to expand our understanding of

730 olivine exposure on important taxa that help drive biogeochemical cycling in the oceans,  
731 particularly experiments to test for ecological effects on processes like competition and trophic  
732 interactions at the community and ecosystem levels. Similar experiments can also be conducted  
733 except with other OAE feedstocks harboring different chemical compositions and more rapid  
734 dissolution timescales (Renforth and Henderson, 2017). Future studies can also focus on  
735 determining how biological processes like photosynthesis, respiration, and organic ligand  
736 production could influence olivine dissolution kinetics and their impacts on carbon dioxide  
737 removal.

738  
739 **Data Availability.** All data and parameters can be found at <https://zenodo.org/record/8157750>.

740  
741 **Author contribution:** D.A.H., F.-X.F., S.J.R., and N.G.W. designed the research; D.A.H., F.-  
742 X.F., S.-C.Y, and S.G.J. performed the research. D.A.H., F.-X.F., S.-C.Y, N.G.W., and S.G.J.  
743 analyzed the data. D.A.H., F.-X.F., S.-C.Y, N.G.W., S.J.R., M.G.A., and S.G.J. wrote the paper.

744  
745 **Competing interests:** Authors D.A.H. and F.-X.F. received research funding from Vesta, PBC.  
746 N.G.W., M.G.A., and S.J.R. are full time employees at Vesta, PBC.

747  
748

749

750

751

752

753

754

755

756

757

758

759

760

761

## References

762 Albright, R., Caldeira, L., Hosfelt, J., Kwiatkowski, L., Maclaren, J. K., Mason, B. M.,  
763 Nebuchina, Y., Ninokawa, A., Pongratz, J., Ricke, K. L., Rivlin, T., Schneider, K., Sesboüé, M.,  
764 Shamberger, K., Silverman, J., Wolfe, K., Zhu, K., and Caldeira, K.: Reversal of ocean  
765 acidification enhances net coral reef calcification, *Nature*, 531, 362–365,  
766 <https://doi.org/10.1038/nature17155>, 2016.

767

768 Bach, L. T., Gill, S. J., Rickaby, R. E. M., Gore, S., and Renforth, P.: CO<sub>2</sub> Removal With  
769 Enhanced Weathering and Ocean Alkalinity Enhancement: Potential Risks and Co-benefits for  
770 Marine Pelagic Ecosystems, *Frontiers in Climate*, 1–21,  
771 <https://doi.org/10.3389/fclim.2019.00007>, 2019.

772

773 Beerling, D. J., Kantzas, E. P., Lomas, M. R., Wade, P., Eufrazio, R. M., Renforth, P., Sarkar, B.,  
774 Andrews, M. G., James, R. H., Pearce, C. R., Mercure, J.-F., Pollitt, H., Holden, P. B., Edwards,  
775 N. R., Khanna, M., Koh, L., Quegan, S., Pidgeon, N. F., Janssens, I. A., Hansen, J., and Banwart,  
776 S. A.: Potential for large-scale CO<sub>2</sub> removal via enhanced rock weathering with croplands,  
777 *Nature*, 1–20, <https://doi.org/10.1038/s41586-020-2448-9>, 2021.

778

779 Bertrand, E. M., Allen, A. E., Dupont, C. L., Norden-Krichmar, T. M., Bai, J., Valas, R., and  
780 Saito, M. A.: Influence of cobalamin scarcity on diatom molecular physiology and identification  
781 of a cobalamin acquisition protein, *Proceedings of the National Academy of Sciences*, E1762–  
782 E1771, <https://doi.org/10.1073/pnas.1201731109/-/dcsupplemental>, 2012.

783

784 Brzezinski, M. A.: THE Si:C:N RATIO OF MARINE DIATOMS: INTERSPECIFIC  
785 VARIABILITY AND THE EFFECT OF SOME ENVIRONMENTAL VARIABLES, *J Phycol*,  
786 21, 347–357, <https://doi.org/10.1111/j.0022-3646.1985.00347.x>, 1985.

787

788 Capone, D. G. and Hutchins, D. A.: Microbial biogeochemistry of coastal upwelling regimes in a  
789 changing ocean, *Nat Geosci*, 6, 711–717, <https://doi.org/10.1038/ngeo1916>, 2013.

790 Caserini, S., Storni, N., and Grosso, M.: The Availability of Limestone and Other Raw Materials  
791 for Ocean Alkalinity Enhancement, *Glob. Biogeochem. Cycles*, 36,  
792 <https://doi.org/10.1029/2021gb007246>, 2022.

793 Coale, T. H., Moosburner, M., Horák, A., Oborník, M., Barbeau, K. A., and Allen, A. E.:  
794 Reduction-dependent siderophore assimilation in a model pennate diatom, *Proceedings of the*  
795 *National Academy of Sciences*, 1–9, <https://doi.org/10.1073/pnas.1907234116>, 2019.

796 Dupont, C. L., Barbeau, K., and Palenik, B.: Ni Uptake and Limitation in Marine *Synechococcus*  
797 Strains, *Appl Environ Microb*, 74, 23–31, <https://doi.org/10.1128/aem.01007-07>, 2008.

798

799 Field, C., Behrenfeld, M., Randerson, J., and Falkowski, P.: Primary production of the biosphere:  
800 integrating terrestrial and oceanic components, *Science*, 281, 237–240, 1998.

801

802 Flipkens, G., Blust, R., and Town, R. M.: Deriving Nickel (Ni(II)) and Chromium (Cr(III))  
803 Based Environmentally Safe Olivine Guidelines for Coastal Enhanced Silicate Weathering,  
804 *Environ Sci Technol*, 55, 12362–12371, <https://doi.org/10.1021/acs.est.1c02974>, 2021.

805

806 Frey, B. E., Riedel, G. F., Bass, A. E., and Small, L. F.: Sensitivity of estuarine phytoplankton to  
807 hexavalent chromium, *Estuar Coast Shelf Sci*, 17, 181–187, [https://doi.org/10.1016/0272-](https://doi.org/10.1016/0272-7714(83)90062-8)  
808 [7714\(83\)90062-8](https://doi.org/10.1016/0272-7714(83)90062-8), 1983.

809

810 Fu, F., Zhang, Y., Bell, P. R. F., and Hutchins, D. A.: PHOSPHATE UPTAKE AND GROWTH  
811 KINETICS OF *TRICHODESMIUM* (CYANOBACTERIA) ISOLATES FROM THE NORTH  
812 ATLANTIC OCEAN AND THE GREAT BARRIER REEF, AUSTRALIA1, *J Phycol*, 41, 62–  
813 73, <https://doi.org/10.1111/j.1529-8817.2005.04063.x>, 2005.

814

815 Fu, F., Tschitschko, B., Hutchins, D. A., Larsson, M. E., Baker, K. G., McInnes, A., Kahlke, T.,  
816 Verma, A., Murray, S. A., and Doblin, M. A.: Temperature variability interacts with mean  
817 temperature to influence the predictability of microbial phenotypes, *Global Change Biol*, 28,  
818 5741–5754, <https://doi.org/10.1111/gcb.16330>, 2022.

819

820 Fu, F. X., Yu, E., Garcia, N. S., Gale, J., Luo, Y., Webb, E. A., and Hutchins, D. A.: Differing  
821 responses of marine N<sub>2</sub> fixers to warming and consequences for future diazotroph community  
822 structure, *Aquatic Microbial Ecology*, 72, 33–46, <https://doi.org/10.3354/ame01683>, 2014.

823

824 Fu, F.-X., Mulholland, M. R., Garcia, N. S., Beck, A., Bernhardt, P. W., Warner, M. E., Sañudo-  
825 Wilhelmy, S. A., and Hutchins, D. A.: Interactions between changing pCO<sub>2</sub>, N<sub>2</sub> fixation, and Fe  
826 limitation in the marine unicellular cyanobacterium *Crocospaera*, *Limnology and*  
827 *Oceanography*, 53, 2472–2484, <https://doi.org/10.4319/lo.2008.53.6.2472>, 2008.

828 Gately, J. A., Kim, S. M., Jin, B., Brzezinski, M. A., and Iglesias-Rodriguez, M. D.:  
829 Coccolithophores and diatoms resilient to ocean alkalinity enhancement: A glimpse of hope?,  
830 *Sci. Adv.*, 9, eadg6066, <https://doi.org/10.1126/sciadv.adg6066>, 2023.

831 Gore, S., Renforth, P., and Perkins, R.: The potential environmental response to increasing ocean  
832 alkalinity for negative emissions, *Mitig. Adapt. Strat. Glob. Chang.*, 24, 1191–1211,  
833 <https://doi.org/10.1007/s11027-018-9830-z>, 2019.

834

835 Guo, J. A., Strzepek, R., Willis, A., Ferderer, A., and Bach, L. T.: Investigating the effect of  
836 nickel concentration on phytoplankton growth to assess potential side-effects of ocean alkalinity  
837 enhancement, *Biogeosciences*, 19, 3683–3697, <https://doi.org/10.5194/bg-19-3683-2022>, 2022.

838

839 Hartmann, J., West, A. J., Renforth, P., Köhler, P., Rocha, C. L. D. L., Wolf-Gladrow, D. A.,  
840 Dürr, H. H., and Scheffran, J.: ENHANCED CHEMICAL WEATHERING AS A  
841 GEOENGINEERING STRATEGY TO REDUCE ATMOSPHERIC CARBON DIOXIDE,  
842 SUPPLY NUTRIENTS, AND MITIGATE OCEAN ACIDIFICATION, *Reviews of Geophysics*,  
843 1–37, <https://doi.org/10.1002/rog.20004>, 2013.

844 Hauck, J., Köhler, P., Wolf-Gladrow, D., and Völker, C.: Iron fertilisation and century-scale  
845 effects of open ocean dissolution of olivine in a simulated CO<sub>2</sub> removal experiment, *Environ.*  
846 *Res. Lett.*, 11, 024007, <https://doi.org/10.1088/1748-9326/11/2/024007>, 2016.

847

848 Hawco, N. J., McIlvin, M. M., Bundy, R. M., Tagliabue, A., Goepfert, T. J., Moran, D. M.,  
849 Valentin-Alvarado, L., DiTullio, G. R., and Saito, M. A.: Minimal cobalt metabolism in the  
850 marine cyanobacterium *Prochlorococcus*, *Proc National Acad Sci*, 117, 15740–15747,  
851 <https://doi.org/10.1073/pnas.2001393117>, 2020.

852

853 He, J. and Tyka, M. D.: Limits and CO<sub>2</sub> equilibration of near-coast alkalinity enhancement,  
854 *Egusphere*, 2022, 1–26, <https://doi.org/10.5194/egusphere-2022-683>, 2022.

855

856 Hutchins, D. A. and Boyd, P. W.: Marine phytoplankton and the changing ocean iron cycle,  
857 *nature climate change*, 6, 1072–1079, <https://doi.org/10.1038/nclimate3147>, 2016.

858

859 Hutchins, D. A. and Sañudo-Wilhelmy, S. A.: The Enzymology of Ocean Global Change, *Annu*  
860 *Rev Mar Sci*, 14, 1–25, <https://doi.org/10.1146/annurev-marine-032221-084230>, 2021.

861

862 Hutchins, D. A., Fu, F.-X., Zhang, Y., Warner, M. E., Feng, Y., Portune, K., Bernhardt, P. W.,  
863 and Mulholland, M. R.: CO<sub>2</sub> control of *Trichodesmium* N<sub>2</sub> fixation, photosynthesis, growth  
864 rates, and elemental ratios: Implications for past, present, and future ocean biogeochemistry,  
865 *Limnol Oceanogr*, 52, 1293–1304, <https://doi.org/10.4319/lo.2007.52.4.1293>, 2007.

866 IPCC: IPCC, 2022: Climate Change 2022: Mitigation of Climate Change. Contribution of  
867 Working Group III to the Sixth Assessment Report of the Intergovernmental Panel on Climate  
868 Change, *Popul. Dev. Rev.*, 48, 629–633, <https://doi.org/10.1017/9781009157926>, 2022.

869

870 Jiang, H.-B., Fu, F.-X., Rivero-Calle, S., Levine, N. M., Sañudo-Wilhelmy, S. A., Qu, P.-P.,  
871 Wang, X.-W., Pinedo-Gonzalez, P., Zhu, Z., and Hutchins, D. A.: Ocean warming alleviates iron  
872 limitation of marine nitrogen fixation, *Nat Clim Change*, 8, 709–712,  
873 <https://doi.org/10.1038/s41558-018-0216-8>, 2018.

874

875 John, S. G., Kelly, R. L., Bian, X., Fu, F., Smith, M. I., Lanning, N. T., Liang, H., Pasquier, B.,  
876 Seelen, E. A., Holzer, M., Wasylenki, L., Conway, T. M., Fitzsimmons, J. N., Hutchins, D. A.,  
877 and Yang, S.-C.: The biogeochemical balance of oceanic nickel cycling, *Nat Geosci*, 15, 906–  
878 912, <https://doi.org/10.1038/s41561-022-01045-7>, 2022.

879 John, S. G., Mendez, J., Moffett, J., and Adkins, J.: The flux of iron and iron isotopes from San  
880 Pedro Basin sediments, *Geochim. Cosmochim. Acta*, 93, 14–29,  
881 <https://doi.org/10.1016/j.gca.2012.06.003>, 2012.

882

883 Karthikeyan, P., Marigoudar, S. R., Nagarjuna, A., and Sharma, K. V.: Toxicity assessment of  
884 cobalt and selenium on marine diatoms and copepods, *Environ Chem Ecotoxicol*, 1, 36–42,  
885 [doi.org/10.1016/j.enceco.2019.06.001](https://doi.org/10.1016/j.enceco.2019.06.001), 2019.

886

887 Kazamia, E., Sutak, R., Paz-Yepes, J., Dorrell, R. G., Vieira, F. R. J., Mach, J., Morrissey, J.,  
888 Leon, S., Lam, F., Pelletier, E., Camadro, J.-M., Bowler, C., and Lesuisse, E.: Endocytosis-  
889 mediated siderophore uptake as a strategy for Fe acquisition in diatoms, *Sci Adv*, 4, eaar4536,  
890 <https://doi.org/10.1126/sciadv.aar4536>, 2018.

891

892 Kiran, B., Rani, N., and Kaushik, A.: Environmental toxicity: Exposure and impact of chromium  
893 on cyanobacterial species, *J Environ Chem Eng*, 4, 4137–4142,  
894 <https://doi.org/10.1016/j.jece.2016.09.021>, 2016.

895

896 Kling, J. D., Kelly, K. J., Pei, S., Rynearson, T. A., and Hutchins, D. A.: Irradiance modulates  
897 thermal niche in a previously undescribed low-light and cold-adapted nano-diatom, *Limnol*  
898 *Oceanogr*, 66, 2266–2277, <https://doi.org/10.1002/lno.11752>, 2021.

899 **Laxen D.P.H., 1985. Trace metal adsorption/coprecipitation on hydrous ferric oxide under**  
900 **realistic conditions: The role of humic substances, *Water Research* 19(10): 1229-1236.**



901  
902 Lee, M. D., Webb, E. A., Walworth, N. G., Fu, F.-X., Held, N. A., Saito, M. A., and Hutchins,  
903 D. A.: Transcriptional Activities of the Microbial Consortium Living with the Marine Nitrogen-  
904 Fixing Cyanobacterium *Trichodesmium* Reveal Potential Roles in Community-Level Nitrogen  
905 Cycling, *Applied and environmental microbiology*, 84, e02026-17–16,  
906 <https://doi.org/10.1128/aem.02026-17>, 2018.

907  
908 Manck, L. E., Park, J., Tully, B. J., Poire, A. M., Bundy, R. M., Dupont, C. L., and Barbeau, K.  
909 A.: Petrobactin, a siderophore produced by *Alteromonas*, mediates community iron acquisition in  
910 the global ocean, *Isme J*, 16, 358–369, <https://doi.org/10.1038/s41396-021-01065-y>, 2022.

911  
912 Meysman, F. J. R. and Montserrat, F.: Negative CO<sub>2</sub> emissions via enhanced silicate weathering  
913 in coastal environments, *Biol Letters*, 13, 20160905, <https://doi.org/10.1098/rsbl.2016.0905>,  
914 2017.

915  
916 Millero, F. J., Sotolongo, S., and Izaguirre, M.: The oxidation kinetics of Fe(II) in seawater,  
917 *Geochim Cosmochim Ac*, 51, 793–801, [https://doi.org/10.1016/0016-7037\(87\)90093-7](https://doi.org/10.1016/0016-7037(87)90093-7), 1987.  
918 Moran, M. A.: The global ocean microbiome, *Science*, 350, aac8455–aac8455,  
919 <https://doi.org/10.1126/science.aac8455>, 2015.

920 Moran, M. A.: The global ocean microbiome, *Science*, 350, aac8455–aac8455,  
921 <https://doi.org/10.1126/science.aac8455>, 2015.

922  
923 Morrissey, J. M. and Bowler, C.: Iron utilization in marine cyanobacteria and eukaryotic algae,  
924 *Frontiers in Microbiology*, 3, 1–13, <https://doi.org/10.3389/fmicb.2012.00043/abstract>, 2012.

925 Oelkers, E. H., Declercq, J., Saldi, G. D., Gislason, S. R., and Schott, J.: Olivine dissolution  
926 rates: A critical review, *Chem Geol*, 500, 1–19, <https://doi.org/10.1016/j.chemgeo.2018.10.008>,  
927 2018.

928  
929 Paasche, E., Brubak, S., Skattebøl, S., Young, J. R., and Green, J. C.: Growth and calcification in  
930 the coccolithophorid *Emiliana huxleyi* (Haptophyceae) at low salinities, *Phycologia*, 35, 394–  
931 403, <https://doi.org/10.2216/i0031-8884-35-5-394.1>, 1996.

932  
933 Panneerselvam, K., Marigoudar, S. R., and Dhandapani, M.: Toxicity of Nickel on the Selected  
934 Species of Marine Diatoms and Copepods, *Bull. Environ. Contam. Toxicol.*, 100, 331–337,  
935 <https://doi.org/10.1007/s00128-018-2279-7>, 2018.

936  
937 Pettine, M., Millero, F. J., and Noce, T. L.: Chromium (III) interactions in seawater through its  
938 oxidation kinetics, *Mar Chem*, 34, 29–46, [https://doi.org/10.1016/0304-4203\(91\)90012-1](https://doi.org/10.1016/0304-4203(91)90012-1), 1991.

939  
940 Reimers, C. E., Stecher, H. A., Taghon, G. L., Fuller, C. M., Huettel, M., Rusch, A., Ryckelynck,  
941 N., and Wild, C.: In situ measurements of advective solute transport in permeable shelf sands,  
942 *Cont Shelf Res*, 24, 183–201, <https://doi.org/10.1016/j.csr.2003.10.005>, 2004.

943  
944 Renforth, P. and Henderson, G.: Assessing ocean alkalinity for carbon sequestration, *Rev*  
945 *Geophys*, 55, 636–674, <https://doi.org/10.1002/2016rg000533>, 2017.

946  
947 Rimstidt, J. D., Brantley, S. L., and Olsen, A. A.: Systematic review of forsterite dissolution rate  
948 data, *Geochim Cosmochim Acta*, 99, 159–178, <https://doi.org/10.1016/j.gca.2012.09.019>, 2012.

949 Rogelj, J., Popp, A., Calvin, K. V., Luderer, G., Emmerling, J., Gernaat, D., Fujimori, S.,  
950 Strefler, J., Hasegawa, T., Marangoni, G., Krey, V., Kriegler, E., Riahi, K., Vuuren, D. P. van,  
951 Doelman, J., Drouet, L., Edmonds, J., Fricko, O., Harmsen, M., Havlík, P., Humpenöder, F.,  
952 Stehfest, E., and Tavoni, M.: Scenarios towards limiting global mean temperature increase below  
953 1.5 °C, *Nat. Clim. Chang.*, 8, 325–332, <https://doi.org/10.1038/s41558-018-0091-3>, 2018.

954  
955 Rubin, M., Berman-Frank, I., and Shaked, Y.: Dust- and mineral-iron utilization by the marine  
956 dinitrogen-fixer *Trichodesmium*, *Nature Geoscience*, 4, 529–534,  
957 <https://doi.org/10.1038/ngeo1181>, 2011.

958  
959 Shi, T., Ilikchyan, I., Rabouille, S., and Zehr, J. P.: Genome-wide analysis of diel gene  
960 expression in the unicellular N<sub>2</sub>-fixing cyanobacterium *Crocospaera watsonii* WH 8501, *Isme*  
961 *J*, 4, 621–632, <https://doi.org/10.1038/ismej.2009.148>, 2010.

962  
963 Sunda, W. G. and Huntsman, S. A.: Cobalt and zinc interreplacement in marine phytoplankton:  
964 Biological and geochemical implications, *Limnol Oceanogr*, 40, 1404–1417,  
965 <https://doi.org/10.4319/lo.1995.40.8.1404>, 1995.

966  
967 Sunda, W. G., Price, N. M., and Morel, F. M. M.: Trace Metal Ion Buffers and Their Use in  
968 Culture Studies, *Algal Culturing Techniques*, 35–63, [https://doi.org/10.1016/b978-012088426-](https://doi.org/10.1016/b978-012088426-1/50005-6)  
969 [1/50005-6](https://doi.org/10.1016/b978-012088426-1/50005-6), 2005.

970 Taylor, L. L., Quirk, J., Thorley, R. M. S., Kharecha, P. A., Hansen, J., Ridgwell, A., Lomas, M.  
971 R., Banwart, S. A., and Beerling, D. J.: Enhanced weathering strategies for stabilizing climate  
972 and averting ocean acidification, *Nat. Clim. Chang.*, 6, 402–406,  
973 <https://doi.org/10.1038/nclimate2882>, 2016.

974

975 Tovar-Sanchez, A., Sañudo-Wilhelmy, S. A., Garcia-Vargas, M., Weaver, R. S., Popels, L. C.,  
976 and Hutchins, D. A.: A trace metal clean reagent to remove surface-bound iron from marine  
977 phytoplankton, *Mar Chem*, 82, 91–99, [https://doi.org/10.1016/s0304-4203\(03\)00054-9](https://doi.org/10.1016/s0304-4203(03)00054-9), 2003.

978

979 Tréguer, P., Bowler, C., Moriceau, B., Dutkiewicz, S., Gehlen, M., Aumont, O., Bittner, L.,  
980 Dugdale, R., Finkel, Z., Iudicone, D., Jahn, O., Guidi, L., Lasbleiz, M., Leblanc, K., Levy, M.,  
981 and Pondaven, P.: Influence of diatom diversity on the ocean biological carbon pump, *Nat*  
982 *Geosci*, 11, 27–37, <https://doi.org/10.1038/s41561-017-0028-x>, 2018.

983

984 Vink, J. P. M. and Knops, P.: Size-Fractionated Weathering of Olivine, Its CO<sub>2</sub>-Sequestration  
985 Rate, and Ecotoxicological Risk Assessment of Nickel Release, *Mineral-basel*, 13, 235,  
986 <https://doi.org/10.3390/min13020235>, 2023.

987

988 Weijden, C. H. V. D. and Reith, M.: Chromium(III) — chromium(VI) interconversions in  
989 seawater, *Mar Chem*, 11, 565–572, [https://doi.org/10.1016/0304-4203\(82\)90003-2](https://doi.org/10.1016/0304-4203(82)90003-2), 1982.

990 Welschmeyer, N. A.: Fluorometric analysis of chlorophyll a in the presence of chlorophyll b and  
991 pheopigments, *Limnol Oceanogr*, 39, 1985–1992, <https://doi.org/10.4319/lo.1994.39.8.1985>,  
992 1994.

993

994 Yamamoto, T., Goto, I., Kawaguchi, O., Minagawa, K., Ariyoshi, E., and Matsuda, O.:  
995 Phytoremediation of shallow organically enriched marine sediments using benthic microalgae,  
996 *Mar Pollut Bull*, 57, 108–115, <https://doi.org/10.1016/j.marpolbul.2007.10.006>, 2008.

997

998 Yang, N., Lin, Y.-A., Merkel, C. A., DeMers, M. A., Qu, P.-P., Webb, E. A., Fu, F.-X., and  
999 Hutchins, D. A.: Molecular mechanisms underlying iron and phosphorus co-limitation responses  
1000 in the nitrogen-fixing cyanobacterium *Crocospaera*, *Isme J*, 16, 2702–2711,  
1001 <https://doi.org/10.1038/s41396-022-01307-7>, 2022.

1002 Yoshida, M., Kuma, K., Iwade, S., Isoda, Y., Takata, H., and Yamada, M.: Effect of aging time  
1003 on the availability of freshly precipitated ferric hydroxide to coastal marine diatoms, *Mar. Biol.*,  
1004 149, 379–392, <https://doi.org/10.1007/s00227-005-0187-y>, 2006.

1005